

# Coherent control of artificial molecules using an Aharonov-Bohm magnetic flux

Matisse Wei-Yuan Tu,<sup>1,2</sup> Wei-Min Zhang,<sup>1,2,\*</sup> and Franco Nori<sup>2,3,†</sup>

<sup>1</sup>*Department of Physics, National Cheng Kung University, Tainan 70101, Taiwan*

<sup>2</sup>*Advanced Science Institute, RIKEN, Saitama 351-0198, Japan*

<sup>3</sup>*Physics Department, The University of Michigan, Ann Arbor, Michigan 48109-1040, USA.*

(Dated: February 28, 2022)

Bonding and anti-bonding states of artificial molecules have been realized in experiments by directly coupling two quantum dots. Without a direct coupling between two nearby quantum dots, here we show that a continuous crossover, from symmetric to anti-symmetric molecular state, can be achieved by changing the flux through a double quantum dot Aharonov-Bohm (AB) interferometer. We explicitly present the flux-dependent real-time processes of molecular-state formation. In contrast to the transport current, which has a  $2\pi$  period, the quantum state of the DQD molecule has a  $4\pi$  period in the AB flux.

PACS numbers: 73.63.Kv, 03.65.Wj

It is important to tailor quantum states, especially, to control the coherent phase between two superposition states. In the past decades, artificial atoms and molecules in solid-state systems, such as superconducting Josephson junctions [1] and semiconductor quantum dots (QDs) [2–4] have provided novel platforms for exploring such quantum-coherent effects. Due to the tunability of various electronic couplings, double quantum dot (DQD) systems, which are archetypes of artificial molecules, have attracted considerable attention. Using direct-tunnel coupling, the coherence of charge states have been investigated with Aharonov-Bohm (AB) interferometers in recent experiments [5, 6]. However, the couplings to the electron reservoirs (electrodes used for measurements and controls), generally induces decoherence to the quantum state of the DQD molecule. Here, we show that for an uncoupled DQD in an AB interferometer, such decoherence can be suppressed with an asymmetric design of the device geometry. Therefore, by solely tuning the AB flux, the coherent control of the DQD molecule (from the symmetric to the anti-symmetric state) can be realized. Furthermore, we find that the period of the quantum state of the DQD in the AB flux is  $4\pi$ . The transport current, obtained by averaging the DQD states, possesses a period of  $2\pi$ . The coherence of the DQD molecular state and the coherence of electron transport therefore manifest themselves fundamentally different through the AB flux.

Coupled DQDs have been theoretically proposed as qubits [7, 8] and experimentally realized [3, 4, 9–12]. The feasibility of realizing various one- and two-electron molecular states with tunable tunneling and exchange couplings was demonstrated [13, 14]. Furthermore, the coherence of electron transport has been investigated with a single QD in AB interferometers [15]. Combining an inter-dot tunnel coupling with a magnetic flux has also been studied theoretically [16–18] and experimentally [5, 6, 19, 20]. In particular, controlling the molecular-state through AB phases is of recent exper-

imental interest [5]. Although tunneling to the electrodes may be turned off to avoid the electron-reservoirs-induced decoherence, such tunnelings are indispensable for the AB effect. Thus controlling the molecular coherence through the AB flux is a new challenge.

Here we consider uncoupled DQDs embedded in an AB interferometer, as sketched in Fig. 1. In contrast to previous theoretical studies, which focus on quantum transport [17, 18], here we directly exploit the quantum state of the artificial molecule. By explicitly analyzing the decoherence through the AB flux, we deduce the proper geometry of the DQD for coherent control over the molecular states. The time-resolved formation processes of various molecular states, determined by different AB fluxes, are explicitly presented.

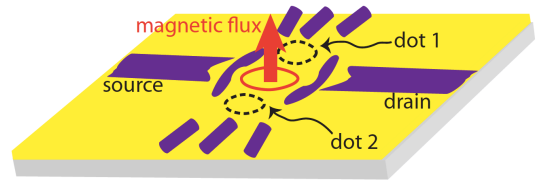


FIG. 1: (color online). A schematic diagram of a pair of uncoupled quantum dots in an Aharonov-Bohm interferometer.

*The model system and its exact solution.*—To focus on the influence of the AB flux on the quantum state of the artificial molecule, we consider only polarized non-interacting electrons. The total Hamiltonian of the system is conventionally [21] given by  $\mathcal{H} = \mathcal{H}_s + \mathcal{H}_E + \mathcal{H}_T$ , in which  $\mathcal{H}_s = \sum_i E_i a_i^\dagger a_i$  describes an uncoupled DQD and  $\mathcal{H}_E = \sum_{\alpha\mathbf{k}} \epsilon_{\alpha\mathbf{k}} c_{\alpha\mathbf{k}}^\dagger c_{\alpha\mathbf{k}}$  is the Hamiltonian for the leads with  $\alpha = L(R)$  labeling the source (drain) lead, and  $\mathcal{H}_T = \sum_{j\alpha\mathbf{k}} [V_{j\alpha} c_{\alpha\mathbf{k}}^\dagger a_j + \text{H.c.}]$  depicts the coupling between the central dot system and the leads. Here  $a_i^\dagger$  ( $a_i$ ) and  $c_{\alpha\mathbf{k}}^\dagger$  ( $c_{\alpha\mathbf{k}}$ ) are the electron creation (annihilation) operators for the electronic levels  $i$  and  $\mathbf{k}$  in the

dot system and the lead  $\alpha$ , respectively. The tunneling amplitudes harbor the applied magnetic flux  $\Phi$  via  $V_{1L}^* = V_{2L} = |V_L|e^{i\phi/4}$ , and  $V_{1R} = V_{2R}^* = |V_R|e^{i\phi/4}$ , where  $\phi = 2\pi\Phi/\Phi_0$  and  $\Phi_0 = h/e$  is the flux quantum. The line-widths induced by tunneling are then given by  $\Gamma_\alpha = 2\pi|V_{j\alpha}|^2\rho_\alpha$ , where  $\rho_\alpha$  is the density of states in the lead  $\alpha$ . The DQD molecular states are governed by the following master equation [22]:

$$\frac{d}{dt}\rho(t) = -i[\mathcal{H}_s, \rho(t)] + \sum_{i\alpha} [\mathcal{L}_{i\alpha}^+(t) + \mathcal{L}_{i\alpha}^-(t)]\rho(t), \quad (1)$$

where  $\mathcal{L}_{i\alpha}^\pm(t)$  are the superoperators describing dissipations and fluctuations induced by the tunnel coupling to the electrodes (for details, see Ref. [22]). Denoting the state of the empty DQD by  $|0\rangle$ , one electron on the first and the second dot by  $|1\rangle$  and  $|2\rangle$ , respectively, and the state of both dots occupied by  $|3\rangle$ , the density matrix  $\rho(t)$  can be generally expressed as

$$\rho(t) = \begin{pmatrix} \rho_{00}(t) & 0 & 0 & 0 \\ 0 & \rho_{11}(t) & \rho_{12}(t) & 0 \\ 0 & \rho_{21}(t) & \rho_{22}(t) & 0 \\ 0 & 0 & 0 & \rho_{33}(t) \end{pmatrix} \quad (2)$$

where  $\rho_{ij} = \langle i|\rho|j\rangle$  with  $i, j = 0, 1, 2, 3$ . The molecular state, featured as one electron in the DQD shared between the two orbitals of the dots, is embedded in the central  $2 \times 2$  block matrix of Eq. (2). In particular, the coherence between the two atomic orbitals of the DQD molecule is characterized by the off-diagonal element,  $\rho_{21}$ . To see how molecular states in this DQD are formed in time, we solve the master equation (1) with the initial preparation of empty DQD, namely,  $\rho_{00}(0) = 1$  and  $\rho_{ij}(0) = 0$ , for all  $i \neq 0, j \neq 0$ . The explicit solution of each matrix element gives

$$\begin{aligned} \rho_{11}(t) &= v_{11}(t) - \det \mathbf{v}(t), \\ \rho_{22}(t) &= v_{22}(t) - \det \mathbf{v}(t), \\ \rho_{12}(t) &= v_{12}(t), \quad \rho_{21}(t) = v_{21}(t), \\ \rho_{00}(t) &= \det[I - \mathbf{v}(t)], \quad \rho_{33}(t) = \det \mathbf{v}(t), \end{aligned} \quad (3)$$

with  $I$  being an identity matrix and

$$\mathbf{v}(t) = \int \frac{d\omega}{2\pi} \mathbf{u}(t, \omega) \sum_{\alpha} f_{\alpha}(\omega) \Gamma_{\alpha} \begin{pmatrix} 1 & e^{\pm i\phi/2} \\ e^{\mp i\phi/2} & 1 \end{pmatrix} \mathbf{u}^{\dagger}(t, \omega) \quad (4)$$

is a  $2 \times 2$  hermitian matrix, where  $f_{\alpha}(\omega)$  is the Fermi distribution function of the reservoirs, the upper (lower) sign is for  $\alpha = L$  ( $R$ ), and  $\mathbf{u}(t, \omega) = \int_{t_0}^t d\tau e^{i\omega(t-\tau)} \mathbf{u}(\tau)$  with

$$\mathbf{u}(\tau) = \exp \left[ - \begin{pmatrix} iE_1 + \Gamma & \Gamma_c(\phi) \\ \Gamma_c^*(\phi) & iE_2 + \Gamma \end{pmatrix} \tau \right]. \quad (5)$$

Here we have defined  $\Gamma_c(\phi) = \Gamma \cos(\phi/2) + i\delta\Gamma \sin(\phi/2)$  with  $\Gamma = \Gamma_L + \Gamma_R$  and  $\delta\Gamma = \Gamma_L - \Gamma_R$ . The functions  $\mathbf{u}(t)$  and  $\mathbf{v}(t)$  are indeed the retarded and correlation Green functions in the Schwinger-Keldysh nonequilibrium Green function theory [23]. The AB flux  $\phi$ , the coupling asymmetry  $\delta\Gamma$ , the non-degeneracy  $\delta E = E_1 - E_2$ , and the nonequilibrium dynamics from the electron tunnelings, all influence the consequent quantum states of the DQD molecule.

*Coherent phases controlled by the AB flux.*— To have a clear picture of the coherence of the DQD molecular state, let us look at the off-diagonal matrix element  $\rho_{12}(t)$  in Eq. (3) first, in the steady-state limit ( $t \gg \Gamma^{-1}$ ). The general solution gives

$$\begin{aligned} \rho_{21} &= \frac{1}{2\pi} \left[ \tan^{-1} \left( \frac{eV}{2\Gamma_+(\phi)} \right) + \tan^{-1} \left( \frac{eV}{2\Gamma_-(\phi)} \right) \right] \left[ \frac{\delta\Gamma}{\Gamma} \cos \frac{\phi}{2} - i \sin \frac{\phi}{2} \right] + \frac{\delta E}{4\pi\gamma(\phi)} \left[ \frac{1}{\Gamma_+(\phi)} \tan^{-1} \left( \frac{eV}{2\Gamma_+(\phi)} \right) \right. \\ &\quad \left. - \frac{1}{\Gamma_-(\phi)} \tan^{-1} \left( \frac{eV}{2\Gamma_-(\phi)} \right) \right] \left\{ \frac{1}{\Gamma} \left[ (\Gamma^2 - \delta\Gamma^2) \sin \frac{\phi}{2} - \delta\Gamma\delta E \cos \frac{\phi}{2} \right] - i\delta E \sin \frac{\phi}{2} \right\}, \end{aligned} \quad (6)$$

where  $\gamma(\phi) = \sqrt{\Gamma^2 \cos^2(\phi/2) + \delta\Gamma^2 \sin^2(\phi/2) - \delta E^2}$  and  $\Gamma_{\pm}(\phi) = 2^{-1}(\Gamma \pm \gamma(\phi))$ . Here, we have also applied a bias  $\mu_L = eV/2 = -\mu_R$  at zero temperature. The full

complexity of decoherence is revealed through Eq. (6). Due to the severe decoherence in such system, it can be proven [24] that the coherent phase  $\varphi$  (in the off-diagonal

matrix element  $\rho_{21} = |\rho_{21}|e^{i\varphi}$  between the two atomic orbitals can only take the values of  $0, \pm\pi/2$  or  $\pi$  for arbitrary flux. This applies for the often-used condition of degeneracy  $\delta E = 0$  and symmetric coupling  $\delta\Gamma = 0$ . The decoherence-induced discretization of the coherent phase hinders the manipulation of the coherent phase of molecular states. However, when the DQD is non-degenerate and couples asymmetrically to the left and the right leads ( $\delta\Gamma \neq 0$ ), we find that the coherent phase  $\varphi$  can be continuously tuned by the AB flux.

In order to achieve typical molecular states, the DQD is set at degeneracy ( $\delta E = 0$ ). The second term in Eq. (6) vanishes. Equations (3,6) show that the formation of molecular states is essentially determined by the applied bias and the coupling asymmetry to the source and the drain. The basic setup of zero bias (which is used for examining quantum transport) leads to  $\rho_{21} = 0$  (because the DQD is in equilibrium with the reservoirs) and is not interested here. With a large bias,  $eV \gg \Gamma$ , we find

$$\rho_{21} = \begin{cases} \frac{1}{2} [(\delta\Gamma/\Gamma) \cos \frac{\phi}{2} - i \sin \frac{\phi}{2}] & \text{if } \phi \neq 0, \\ \frac{1}{4}(1 + \delta\Gamma/\Gamma) & \text{if } \phi = 0. \end{cases} \quad (7)$$

Equation (7) clearly shows the controllability of the coherent phase between the two atomic orbitals of the DQD molecule through the AB flux. It also explicitly reveals the necessity of the asymmetry in couplings,  $\delta\Gamma \neq 0$ . In the case of symmetric coupling,  $\delta\Gamma = 0$ , Eq. (7) shows that the real part vanishes for  $\phi \neq 0$  so that the coherent phase  $\varphi$  is localized at  $\pi/2$ , except for  $\phi = 0$  where the coherence phase is restricted to 0, as it has been pointed out in [24]. With the larger asymmetry  $\delta\Gamma$ , the coherence amplitude  $|\rho_{21}|$  linearly increases and the coherence phase is continually driven by the AB flux, as seen from Eq. (7) [25]. By setting  $\delta\Gamma \lesssim \Gamma$ , we obtain  $\rho \approx |\psi(\phi)\rangle\langle\psi(\phi)|$ , where

$$|\psi(\phi)\rangle = \frac{1}{\sqrt{2}} [ |1\rangle + \exp(-i\phi/2)|2\rangle ]. \quad (8)$$

A continuous transition from the symmetric,  $|\psi(0)\rangle = (|1\rangle + |2\rangle)/\sqrt{2}$ , to the anti-symmetric state,  $|\psi(\pm 2\pi)\rangle = (|1\rangle - |2\rangle)/\sqrt{2}$ , is achieved by changing the AB flux, as shown in Fig. 2 (see captions). Interestingly we find that the period of the state of the DQD molecule is  $4\pi$ , rather than  $2\pi$  in the AB flux as one expected.

*Real-time processes of molecular-state formations.*—

The full information of the quantum state of the DQD molecule at finite temperature is depicted by the time-dependent reduced density matrix. We can write the central block matrix of Eq. (2) as

$$\rho_q(t) = \frac{1}{2} [I + \mathbf{r}(t) \cdot \boldsymbol{\sigma}] - \frac{1}{2} [\rho_{00}(t) + \rho_{33}(t)]I, \quad (9)$$

where  $\boldsymbol{\sigma} = (\sigma_x, \sigma_y, \sigma_z)$  consists of the Pauli matrices and  $\mathbf{r}(t) = 2\{\text{Re}\rho_{21}(t), \text{Im}\rho_{21}(t), \rho_{11}(t) - \rho_{22}(t)\}$ , is the polarization vector for the molecular states. So the dynamics of molecular-state formations can be visualized

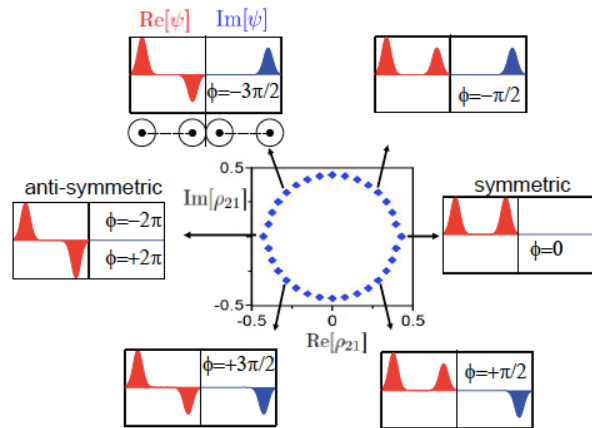


FIG. 2: (color online). Control of the coherent phase of the DQD molecule by the AB flux. The explicit solution of  $\rho_{21}$  in the steady-state limit is shown by the “blue diamonds” on the central panel. Each diamond corresponds to an AB flux value, taken from  $\phi = 0$  to  $\phi = \pm 2\pi$  with  $\pi/8$  steps. The wavefunctions on the DQD molecules are illustrated for various values of the AB flux. A DQD is indicated by two circles with centers connected by a dashed line (no inter-dot coupling) below the diagrams for  $\phi = -3\pi/2$ . Both the real (red) and the imaginary (blue) parts are shown, so one sees how the AB flux changes the coherent phase between the atomic orbitals. Other parameters are  $\delta E = 0$ ,  $eV = 6\Gamma$  at  $k_B T = \Gamma/20$ , which are also used in the following figures, unless specified.

through the motion of the polarization vector with the Bloch sphere. Also, the leakage out of the one-electron state-space can be easily seen from the term proportional to the probability of the empty and the double occupied states,  $\rho_{00}(t) + \rho_{33}(t)$ .

In Fig. 3, we plot the evolution of the full reduced density matrix of the DQD molecule. Initially, the DQD is prepared in an empty state,  $\rho_{00}(0) = 1$  as shown by Fig. 3(b1,c1,d1) and  $\mathbf{r}(0) = 0$  given in Fig. 3(a1) (where the length of the red strip is zero). After injecting electrons from the left and the right reservoirs,  $\rho_{00}$  decreases [see Fig. 3(b1) to (b3)] while the electron occupation and coherence increase with time [see plots (b1) to (b3), (c1) to (c3), and also (d1) to (d3) in Fig. 3]. The coherent phase  $\varphi$  between the atomic orbitals has been fixed shortly after the electron injection [see Fig. 3(a1) to (a4) and also (d2) to (d4)]. Then  $|\mathbf{r}(t)|$  grows in time with fixed  $\varphi$ , and finally a stable molecular state,  $\rho \approx |\psi\rangle\langle\psi|$ , where  $|\psi\rangle = (|1\rangle + e^{-i\phi/2}|2\rangle)/\sqrt{2}$ , is reached in a short time, of about  $3\Gamma^{-1}$ . Note that due to possible leakage, see Fig. 3(b3) where  $\rho_{00}$  has a small finite value, the DQD is not in a perfect pure state. But the situation can be optimized by changing the bias and the coupling asymmetry, as shown by Eq. (7).

To better understand the role played by the AB flux, we show the time evolutions of  $\rho_{21}$  in Fig. 4 under various values of  $\phi$ . Figure 4(a1,a2) show the process of coherence generation for a strong asymmetric coupling (with

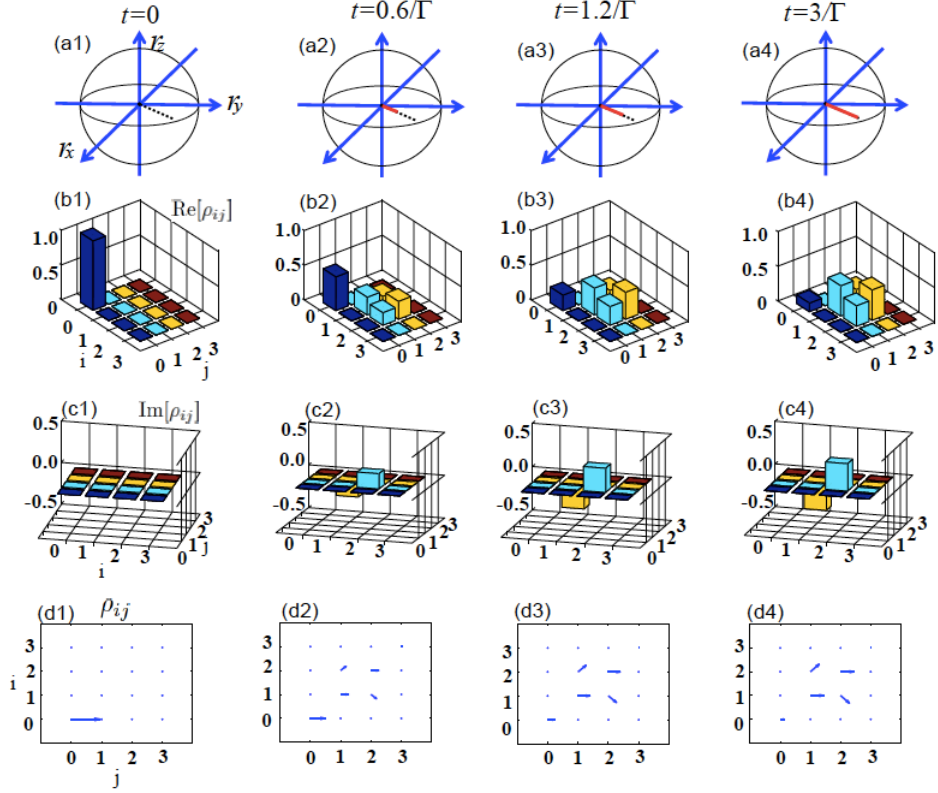


FIG. 3: (color online). Typical process for forming molecular states. The dashed black line in (a1) to (a4) is the trajectory taken by  $\mathbf{r}(t)$  from  $t = 0$  in (a1), starting from the origin, to  $t = 3/\Gamma$  in (a4), where it almost touches the surface of the sphere. The red strip in each plot is the trajectory up to the corresponding time points, as shown above the spheres. From the trajectory, we see the coherent phase  $\varphi$  (which is the angle made by  $\mathbf{r}(t)$  with  $r_x$  axis) has been fixed after the electron is injected into the DQD. Plots (b1) to (b4) display the real part of the reduced density matrix of the DQD system, while the imaginary part is plotted in (c1) through (c4). The coherent phase  $\varphi$  between the two atomic orbitals is better visualized through the vector plots (d1) to (d4). Every arrow represents an element of the reduced density matrix  $\rho_{ij}$ , whose horizontal projection stands for the real part and the vertical projection stands for the imaginary part. The AB flux here is  $\phi = -\pi/2$ .

$\delta\Gamma = 0.9\Gamma$ ). The rate of approaching steady-coherent-molecular states is only weakly dependent on the flux. The stable molecular states are soon reached after a few  $\Gamma^{-1}$ . This is totally different from the symmetric coupling ( $\delta\Gamma = 0$ ), see Fig. 4(b1,b2). It shows the flux-dependent decays of  $\text{Re}\rho_{21}$ , due to the severe decoherence in the symmetric coupling. Therefore, the coupling asymmetry can strongly suppress the decoherence induced by electron tunnelings, and make the coherence control of the QDQ molecule feasible.

*Discussions.*— The general solution shows that the quantum state of the DQD molecule has a period of  $4\pi$  in the AB flux. It is an intrinsic property of this pseudo-spin system, independent of the coupling geometry and the bias configurations. Besides, we have also calculated the tunneling current to reservoir  $\alpha = L, R$  within the same framework [22] with the result  $I_\alpha(t) = e \sum_i \text{tr}_s[\mathcal{L}_{i\alpha}^+(t)\rho(t)]$ . The steady-state transport current

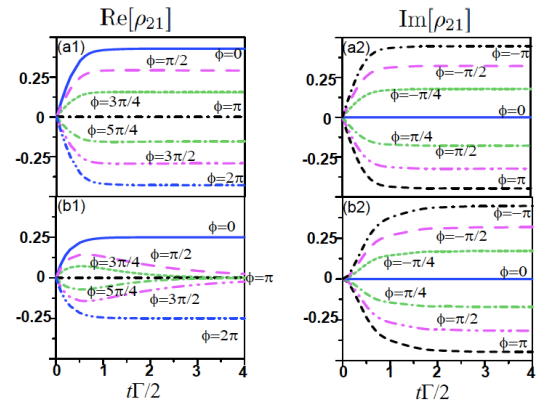


FIG. 4: (color online). The time evolutions of  $\rho_{21}$ . The plots (a1,a2) for  $\delta\Gamma = 0.9\Gamma$  and (b1,b2) for  $\delta\Gamma = 0$ . Also (a1,b1) give  $\text{Re}\rho_{21}$ , and (a2,b2) give  $\text{Im}\rho_{21}$ .

$I = \frac{1}{2}(I_L - I_R)$  is then given by

$$I(\phi) = \int \frac{d\omega}{2\pi} [f_L(\omega) - f_R(\omega)] \mathcal{T}(\omega, \phi), \quad (10)$$

where the transmission coefficient is given by

$$\mathcal{T}(\omega, \phi) = \frac{(\Gamma^2 - \delta\Gamma^2)[\omega^2 \cos^2 \frac{\phi}{2} + \frac{1}{4}\delta E \sin^2 \frac{\phi}{2}]}{[\omega^2 + \Gamma_+^2(\phi)][\omega^2 + \Gamma_-^2(\phi)]}. \quad (11)$$

By taking  $\delta\Gamma = 0$  it reproduces the result in Ref. [21]. Equation (11) clearly shows that the transport current has a period in the AB flux of  $2\pi$ . This  $2\pi$  period, as a feature for the coherence of transport, is well known and has been observed in experiments [15, 19, 20]. The  $4\pi$  period, a nontrivial character of the quantum state of the DQD molecule, requires further experimental investigation. Note that although the coherent phase of the off-diagonal density matrix element is gauge-dependent, the AB flux dependence of the coherence phase and its periodicity are both independent of the gauge choice.

In summary, we have demonstrated the effectiveness of the AB flux for the coherence control of DQD artificial molecules. We have analyzed the AB flux-dependent coherence controlling, through the asymmetric coupling of the DQD to the electron reservoirs. When a large bias is applied with a strong asymmetry in couplings to the source and the drain, coherent control by the AB flux can be easily achieved. The decoherence induced by the electron tunnelings can be efficiently suppressed. We also find that the period of the quantum state of the DQD molecule in the AB flux is  $4\pi$ . The revelation of the underlying quantum-coherence of the molecular states is thus beyond the usual transport measurement. The verifications of these molecular states would rely on a suitable quantum-state-tomography protocol for further investigations. We hope that this theory for artificial molecules could inspire new experiments on coherence control of molecular states via the AB flux, and become also useful for the quantum emulation [26] of artificial molecular processes.

This work is supported in part by the National Science Council of ROC under Contract No. NSC-99-2112-M-006-008-MY3 and we acknowledge support of computing facility from HPC center of national Cheng Kung university and National Center for Theoretical Science. FN is partially supported by the ARO, NSF grant No. 0726909, JSPS-RFBR contract No. 12-02-92100, Grant-in-Aid for Scientific Research (S), MEXT Kakenhi on Quantum Cybernetics, and the JSPS via its FIRST program.

<sup>†</sup> Electronic address: fnori@riken.jp

- [1] J. Q. You and F. Nori, Nature **474**, 590 (2011); Phys. Today **58**, 42 (2005).
- [2] R. Hanson, L. P. Kouwenhoven, J. R. Petta, S. Tarucha, and, L. M. K. Vandersypen, Rev. Mod. Phys. **79**, 1217 (2007).
- [3] I. Buluta, S. Ashhab and F. Nori, Rep. Prog. Phys., **74**, 104401 (2011).
- [4] J. J. L. Morton, D. R. McCamey, M. A. Eriksson, and S. A. Lyon, Nature **479**, 345 (2011).
- [5] T. Hatano, T. Kubo, Y. Tokura, S. Amaha, S. Teraoka, and S. Tarucha, Phys. Rev. Lett. **106**, 076801 (2011).
- [6] M. Yamamoto, S. Takada, C. Bauerle, K. Watanabe, A. D. Wieck and S. Tarucha, Nat. Nanotech. **7**, 247 (2012).
- [7] D. Loss and D. P. DiVincenzo, Phys. Rev. A **57**, 120 (1998).
- [8] R. H. Blick and H. Lorenz, in *Proceedings of the IEEE International Symposium on Circuits and Systems*, edited by J. Calder (IEEE, Piscataway, NJ, 2000), Vol. II, p. 245.
- [9] T. Hayashi, T. Fujisawa, H. D. Cheong, Y. H. Jeong, and Y. Hirayama, Phys. Rev. Lett. **91**, 226804 (2003);
- [10] J. Gorman, D. G. Hasko, and D. A. Williams, Phys. Rev. Lett. **95**, 090502 (2005).
- [11] J. R. Petta, A. C. Johnson, J. M. Taylor, E. A. Laird, A. Yacoby, M. D. Lukin, C. M. Marcus, M. P. Hanson, A. C. Gossard. Science **309**, 1280 (2005).
- [12] K. D. Petersson, J. R. Petta, H. Lu, and A. C. Gossard, Phys. Rev. Lett., **105**, 246804 (2010).
- [13] A. W. Holleitner, R.H. Blick, A.K. Huttel, K. Eberl, and J. P. Kotthaus, Science **297**, 70 (2002).
- [14] T. Hatano, M. Stopa, and S. Tarucha, Science **309**, 268 (2005).
- [15] A. Yacoby, M. Heiblum, D. Mahalu, and H. Shtrikman, Phys. Rev. Lett. **74**, 4047 (1995).
- [16] D. Loss and E.V. Sukhorukov, Phys. Rev. Lett. **84**, 1035 (2000).
- [17] K. Kang and S. Y. Cho, J. Phys. Condens. Matter **16**, 117 (2004).
- [18] T. Kubo, Y. Tokura, T. Hatano, and S. Tarucha, Phys. Rev. B **74**, 205310 (2006).
- [19] A. W. Holleitner, C. R. Decker, H. Qin, K. Eberl, and R. H. Blick, Phys. Rev. Lett. **87**, 256802 (2001).
- [20] M. Sigrist, T. Ihn, K. Ensslin, D. Loss, M. Reinwald, and W. Wegscheider, Phys. Rev. Lett. **96**, 036804 (2006).
- [21] B. Kubala and J. König, Phys. Rev. B **65**, 245301 (2002).
- [22] M. W. Y. Tu and W. M. Zhang, Phys. Rev. B **78**, 235311 (2008); J. S. Jin, M. W. Y. Tu, W. M. Zhang, and Y. J. Yan, New J. Phys. **12**, 083013 (2010).
- [23] J. Schwinger, J. Math. Phys. **2**, 407 (1961); L. V. Keldysh, Sov. Phys. JETP, **20**, 1018 (1965).
- [24] M. W. Y. Tu, W. M. Zhang, and J. S. Jin, Phys. Rev. B **83**, 115318 (2011).
- [25] When  $\phi = 0$ , the amplitude enhancement of the coherence is determined by the sign of  $\delta\Gamma$ . When  $\mu_L > \mu_R$ , the asymmetry of  $\Gamma_L > \Gamma_R$  is preferred for larger  $|\rho_{21}|$ .
- [26] I. Buluta and F. Nori, Science **326**, 108 (2009).

\* Electronic address: wzhang@mail.ncku.edu.tw